Check for updates

Reaction of size-selected iron-oxide cluster cations with methane: a model study of rapid methane loss in Mars' atmosphere†

Masashi Arakawa, [ID] ‡*[a] Satoshi Kono,[a] Yasuhito Sekine [ID] [b] and Akira Terasaki [ID] *[a]

We report gas-phase reactions of free iron-oxide clusters, $Fe_nO_m^+$, and their Ar adducts with methane in the context of chemical processes in Mars' atmosphere. Methane activation was observed to produce $Fe_nO_mCH_2^+/Fe_nO_mCD_2^+$ and $Fe_nO_mC^+$, where the reactivity exhibited size and composition dependence. For example, the rate coefficients of methane activation for Fe_3O^+ and Fe_4O^+ were estimated to be 1×10^{-13} and 3×10^{-13} cm^3 s^{-1}, respectively. Based on these reaction rate coefficients, the presence of iron-oxide clusters/particles with a density as low as 10^7 cm^{-3} in Mars' atmosphere would explain the rapid loss of methane observed recently by the Curiosity rover.

1 Introduction

Clusters of metals and metal compounds are a group of substances with a variety of potential applications taking advantage of their size-specific properties. Among the numerous cluster studies, one of the most intriguing topics is cluster chemistry in space. Small mineral particles such as silicate (*e.g.*, pyroxene (Mg, Fe)SiO$_3$ and olivine (Mg, Fe)$_2$SiO$_4$) are among the most abundant materials in space.[1,2] It is a prevalent hypothesis that such materials contribute to chemical processes in the planet-forming regions, *e.g.*, formation of organic molecules.[3] Size-selected gas-phase clusters provide a good model for this chemistry because it is possible to investigate reactions step by step with precise control over the number of atoms and molecules involved in the reaction,[4–6] providing molecular-level insights into metal- and metal compound-mediated catalytic reactions.[7] Furthermore, spectroscopic studies in laboratories have been reported for silica and silicate clusters,[8–10] which were recently suggested to be highly abundant in the interstellar medium.[8,9] Therefore, clusters themselves may play important roles in chemical processes in space. In this context, we have reported reactions of gas-phase free silicate, $Mg_lSiO_m^-$, and

silica, $Si_nO_m^-$, cluster anions with CO and H_2O molecules.[11,12] In addition, coadsorption and subsequent reaction of CO and H_2 molecules on cobalt cluster cations, Co_n^+, have been examined to discuss the formation of organic molecules on the clusters.[13]

Another chemical process among recent topics in space is rapid methane loss in the atmosphere of Mars.[14] Observation by the Curiosity rover found temporary spikes of methane and its rapid loss, but the mechanism of the loss has not been elucidated yet. Although some previous studies suggested a very local, small methane source near the landing site of the Curiosity rover,[15,16] an alternative possibility is the effective loss of methane *via* chemical reaction that is not considered in photochemical models. Mars' soil is rich in iron oxides, where storms of iron-oxide particles (dust devils) occur very frequently.[17] Hypervelocity impacts of small bodies on Mars would have also evaporated or made molten the surface materials.[18] These surface processes may have formed very fine iron-bearing condensates on Mars. We thus hypothesize that iron-oxide particles/clusters, which are speculated to be abundant on Mars, are responsible for the rapid loss because the diiron-oxide cluster, Fe_2O_2, is known as an active center of methane monooxygenase (sMMO),[19–23] an enzyme that oxidizes C–H bonds in methane.

The C–H dissociation energy of methane is much larger than those of other alkanes as can be expected from its short bond length and the large HOMO–LUMO gap.[24] Numerous theoretical studies on the interaction of methane with model complexes involving a diiron-oxide core have been reported because methane activation is receiving considerable interest in modern chemistry.[25–36] These theoretical studies have revealed that the diiron-oxide core in sMMO plays an important role in C–H bond cleavage. Several mechanisms have been proposed for the hydroxylation of CH_4,[24,34,35] such as a mechanism *via* a CH_3

[a] Department of Chemistry, Faculty of Science, Kyushu University, 744 Motooka, Nishi-ku, Fukuoka 819-0395, Japan. E-mail: arakawa@chem.kyushu-univ.jp, terasaki@chem.kyushu-univ.jp

[b] Earth-Life Science Institute (ELSI), Tokyo Institute of Technology, 2-12-1 Ookayama, Meguro-ku, Tokyo 152-8550, Japan. E-mail: sekine@elsi.jp

† Electronic supplementary information (ESI) available. See DOI: https://doi.org/10.1039/d4cp01337a

‡ Present address: Department of Earth and Planetary Sciences, Faculty of Science, Kyushu University, 744 Motooka, Nishi-ku, Fukuoka 819-0395, Japan. E-mail: arakawa@geo.kyushu-u.ac.jp

14684 | *Phys. Chem. Chem. Phys.*, 2024, **26**, 14684–14690

This journal is © the Owner Societies 2024

radical,[28,29,31] one not *via* radicals[26,27,33,35] and a non-synchronous concerted one.[32]

As for experimental studies, gas-phase free FeO$^+$ was reported to mediate the activation of methane.[37–41] Hydroxylation of methane by FeO$^+$ was suggested to occur *via* a hydroxy intermediate HO–Fe$^+$–CH$_3$.[37,38] This reaction mechanism has been supported by theoretical studies, where the pathway *via* the hydroxy intermediate is energetically more favorable than the one *via* a methoxy intermediate H–Fe$^+$–OCH$_3$.[42,43] The methoxy intermediate was investigated experimentally by vibrational spectroscopy.[44] The reaction was also reported to be accompanied by spin inversion.[45–49] An activation mechanism of methane by neutral FeO and anionic FeO$^-$ as well as cationic FeO$^+$ was theoretically reported recently.[50]

As for multinuclear species, an iron-oxide cluster, Fe$_2$O$_3$,[51] as well as iron clusters, Fe$_2$,[52] Fe$_2^+$[53] and Fe$_4$,[54] has been reported to show methane activation by theory. Furthermore, a number of theoretical studies present geometric and electronic structures of iron-oxide clusters such as FeO$^+$,[55,56] FeO$_2^-$,[57] FeO$_2^{+/0/-}$,[58] FeO$_n^{+/-}$,[59] Fe$_n$O$_m^-$ (n = 3, 4),[60] Fe$_n$O$_m^-$ (n = 1, 2, $m \leq 6$),[61] Fe$_n$O$_m$ (n = 1–5),[62] (FeO)$_n$ (n = 2–5),[63] (FeO)$_n$ ($n >$ 10),[64] (Fe$_2$O$_3$)$_n$ (n = 1–6, 10),[65–67] (Fe$_3$O$_4$)$_n$ (n = 1–5),[68] Fe$_n$O$_m^+$ (n = 3–6),[69] Fe$_n$O$_m$ (n = 33, 45, 113),[70] Fe$_3$O$_{18}$,[71–73] Fe$_{25}$O$_{30}$ and Fe$_{33}$O$_{32}$.[73] However, in contrast to these extensive theoretical studies, experimental reports are limited: geometric-structure studies of (FeO)$_n^+$ (n = 2–9) by ion mobility mass spectrometry[74] and stability studies by photodissociation,[75] collision-induced dissociation[76] and mass spectrometry.[65,71] In particular, reaction with methane has been examined by experiment only for Fe$_2$O$_2^+$.[77] Note that, because methane activation has been attracting strong attention, a significant number of methane-reaction experiments have been reported for metal and metal-compound clusters, including Fe$_n^+$ (n = 2–15),[78] Ni$_n^+$ (n = 2–15),[79] Rh$_n^+$,[80] Pd$_n^+$,[81–83] Ta$_n^+$,[84] Au$_2^+$,[81,82,85,86] FeC$_6^-$,[87] W$_n$C$_m^+$ (n =1–5, $m \leq$ 5),[88] W$_n$N$_m^+$ (n = 1–6, $m \leq$ 2),[88] Al$_2$O$_7^+$,[89] Al$_4$O$_6^+$ and NiAl$_3$O$_6^+$,[90] as well as vibrational spectroscopy of methane complexes with Fe$_n^+$,[91–93] Cu$_n^+$,[94] Ta$_4^+$,[95] Pt$_n^+$[96] and Au$_2^+$.[97]

On the basis of these backgrounds, the present study reports gas-phase reaction of size-selected iron-oxide cluster cations, Fe$_n$O$_m^+$, with methane, CH$_4$, and deuterated methane, CD$_4$, to verify our hypothesis that iron-oxide particles/clusters are responsible for the rapid loss of methane in Mars' atmosphere.

2 Methods

Experiments were performed using the setup described in detail previously.[98,99] Briefly, Fe$_n$O$_m^+$ (n = 2–4, 0 $\leq m \leq n$) were generated by a magnetron-sputter cluster-ion source,[100] with sputtering of an iron plate (Kojundo Chem. Lab. Co., Ltd, 99.99%) in the presence of oxygen (99.99995%). After thermalization by collisions with helium gas at liquid-nitrogen temperature, the generated cluster cations were mass-selected with a quadrupole mass filter (MAX-4000, Extrel CMS, LLC); among the isotopologues for a given composition, the one with the highest abundance was selected. Note that the reactant cluster

cations thus mass-selected contained a trace amount of an Ar adduct Fe$_{n-1}$O$_{m+1}$Ar$^+$ as well, which has the same mass as Fe$_n$O$_m^+$. The cluster cations were introduced into a reaction cell with a linear 40-cm-long rf quadrupole ion guide, where methane (CH$_4$ or deuterated CD$_4$) gas was continuously flowed at 298 K. Ions produced by reaction while passing through the cell were identified by a second quadrupole mass analyzer (MAX-4000, Extrel CMS, LLC) employing a channel electron multiplier (Channeltron 4720, Burle Electro-Optics, Inc.) for an ion detector to measure the yield of each product ion.

The partial pressure of CH$_4$ and CD$_4$ in the reaction cell was adjusted to be 0.1 Pa; the pressure was monitored outside the reaction cell by a residual gas analyzer (RGA100, Stanford Research Systems, Inc.) and was converted to the pressure inside the reaction cell in a way reported previously by referring to the reaction cross section of Cr$_2^+$ with O$_2$.[101,102] The pressure corresponds to the collision rate of 2 × 10^4 s^{-1}, where the collisional cross section is estimated by the Langevin–Giou-mousis–Stevenson model,[103]

$$\sigma = \pi e \{2\alpha/(4\pi\varepsilon_0)^2 E\}^{1/2} \tag{1}$$

Here, α is the polarizability of methane (2.56 Å^3), e is the elementary charge, ε_0 is the vacuum dielectric constant, k is Boltzmann's constant, T is the temperature and E is the collision energy in the center-of-mass frame. The collision energy of the clusters with a methane molecule was 12 eV in the laboratory frame.

3 Results and discussion

3.1 Reaction products

Fig. 1 shows mass spectra of ions upon reaction of Fe$_3$O$_m^+$ (m = 0–3) with deuterated methane, CD$_4$; note that Fe$_2$O$_{m+1}$Ar$^+$, which is coincident in mass with Fe$_3$O$_m^+$, coexists in the reactant in our present experimental conditions. For m = 0, 1 and 3, mass spectra of ions upon reaction with CH$_4$ are also shown (panels a′, b′ and d′). The abscissa shows a mass shift, ΔM, from Fe$_3$O$_m^+$; the peaks observed at $\Delta M \geq 0$ are assigned to ions produced from Fe$_3$O$_m^+$, whereas those at $\Delta M < 0$ are from Fe$_2$O$_{m+1}$Ar$^+$ subject to desorption of an Ar atom. Note also that the mass spectra were not recorded in the vicinity of ΔM = 0 because the intensity of the reactant ion was much higher than those of product ions, which caused saturation in the ion detector; the peak at ΔM = −40, which should have been observed in panels a, a′, b and b′, was also excluded from recording by the same reason.

For the $\Delta M \geq 0$ region manifesting reaction channels from Fe$_3$O$_m^+$, peaks at ΔM = 12 and 16 are observed upon reaction with CD$_4$ as shown in Fig. 1a–d (m = 0–3), while ΔM = 12 and 14 are observed for CH$_4$ as shown in Fig. 1a′, b′ and d′ (m = 0, 1 and 3). These results suggest that Fe$_3$O$_m$C$^+$ and Fe$_3$O$_m$CD$_2^+$/Fe$_3$O$_m$CH$_2^+$ are produced upon reaction, *i.e.*, dehydrogenation from methane proceeds. Mass spectra upon the reaction of Fe$_2$O$_m^+$ (m = 0–2) and Fe$_4$O$_m^+$ (m = 0–3) with CD$_4$ are shown in the $\Delta M \geq 0$ region of Fig. 2, where methane activation to

This journal is © the Owner Societies 2024

Phys. Chem. Chem. Phys., 2024, **26**, 14684–14690 | **14685**

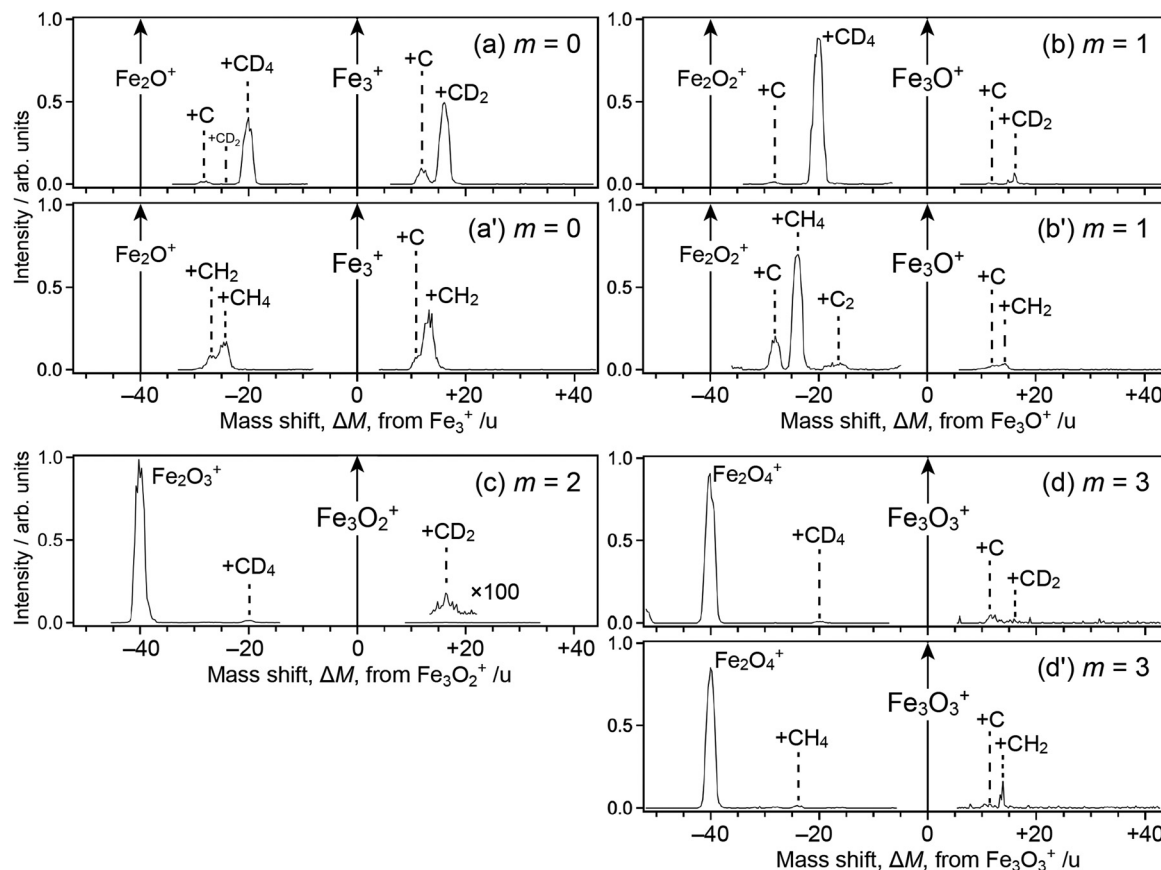**Fig. 1** Mass spectra of ions produced from the reaction of $Fe_3O_m^+$ and $Fe_2O_{m+1}Ar^+$ with (a)–(d) CD_4 or (a′, b′ and d′) CH_4. Reactant ions are $m = 0, 1, 2$ and 3 for (a) and (a′), (b) and (b′), (c) and (d) and (d′), respectively. The abscissa shows a mass shift, ΔM, from $Fe_3O_m^+$. Peaks are assigned to adducts to $Fe_3O_m^+$ in the $\Delta M \geq 0$ region, while adducts to $Fe_2O_{m+1}^+$ after desorption of Ar in the $\Delta M < 0$ region. Note that the following ions are excluded from recording due to saturation: Fe_3^+ and Fe_2O^+ in panels (a) and (a′), Fe_3O^+ and $Fe_2O_2^+$ in (b) and (b′), $Fe_3O_2^+$ in (c) and $Fe_3O_3^+$ in (d) and (d′).

produce $Fe_nO_mC^+$ and/or $Fe_nO_mCD_2^+$ is observed as in the case of $Fe_3O_m^+$. Note that Fe_2O^+ and $Fe_2O_2^+$ are exceptions; reaction products are hardly identified. In the reaction of $Fe_4O_2^+$ and $Fe_4O_3^+$, partially dehydrogenated products, $Fe_4O_mCD_3^+$, are observed.

As for the $\Delta M < 0$ region in Fig. 1, product ions from $Fe_2O_{m+1}Ar^+$ are observed, where the major reaction channel is methane adsorption without dehydrogenation. For example, $Fe_2O_{m+1}CD_4^+$ along with a small amount of $Fe_2O_{m+1}C^+$ is observed in the reaction of $Fe_2O_{m+1}Ar^+$ ($m = 0, 1$), as shown in Fig. 1a and b. Adsorption of CD_4 is accompanied by desorption of an Ar atom to form $Fe_2O_{m+1}CD_4^+$. This is in contrast to the fact that no products are observed in the reaction of Fe_2O^+ and $Fe_2O_2^+$ (see Fig. 2b and c). The results suggest that the adsorption energy of CD_4 was released by the desorption of Ar, which stabilized the CD_4 adducts to survive longer. The peak at $\Delta M = -20$ observed in Fig. 2a and b is also assigned to CD_4 adducts accompanied by Ar desorption from $FeOAr^+$ and FeO_2Ar^+. In particular, the result of $FeOAr^+$ is in contrast to a previous study, which reported that the reaction of FeO^+ with CD_4 proceeds along two reaction channels: either to $FeOD^+ + CD_3$ or to $Fe^+ + CD_3OD$.[37] This would also be due to stabilization of the CD_4 adduct by desorption of Ar as discussed in the previous

reaction study of $Rh_n^+Ar_m$ with CH_4;[80] it was reported that the CH_4 adducts do not have a sufficient energy for activation of the C–H bond due to energy release by ligand exchange.

3.2 Rate coefficients of methane activation

The reaction-rate coefficients to produce the ions described above were estimated in the same way as reported previously[12] by assuming pseudo-first-order reaction kinetics because the density of methane can be treated as constant during the reaction. However, the peak intensity of the reactant is necessary to estimate the rate coefficients, which is missing in the present measurement due to saturation. We therefore performed additional recording of mass spectra with lower sensitivity of the ion detector, where only major peaks, such as those at $\Delta M = 0$ and -40, were observed (see Fig. S1 of the ESI†). The rate coefficients were estimated by combining the relative intensities of the reactant and product ions obtained in this low-sensitivity mode with the intensity ratios of the product ions in Fig. 1 and 2 obtained in a high-sensitivity mode.

Fig. 3 shows rate coefficients thus evaluated for methane dehydrogenation of $Fe_nO_m^+$ in the size range of $n = 2–4$, which summed up all the reaction channels to the formation of C, CD_2 and CD_3 adducts. The result suggests that larger and
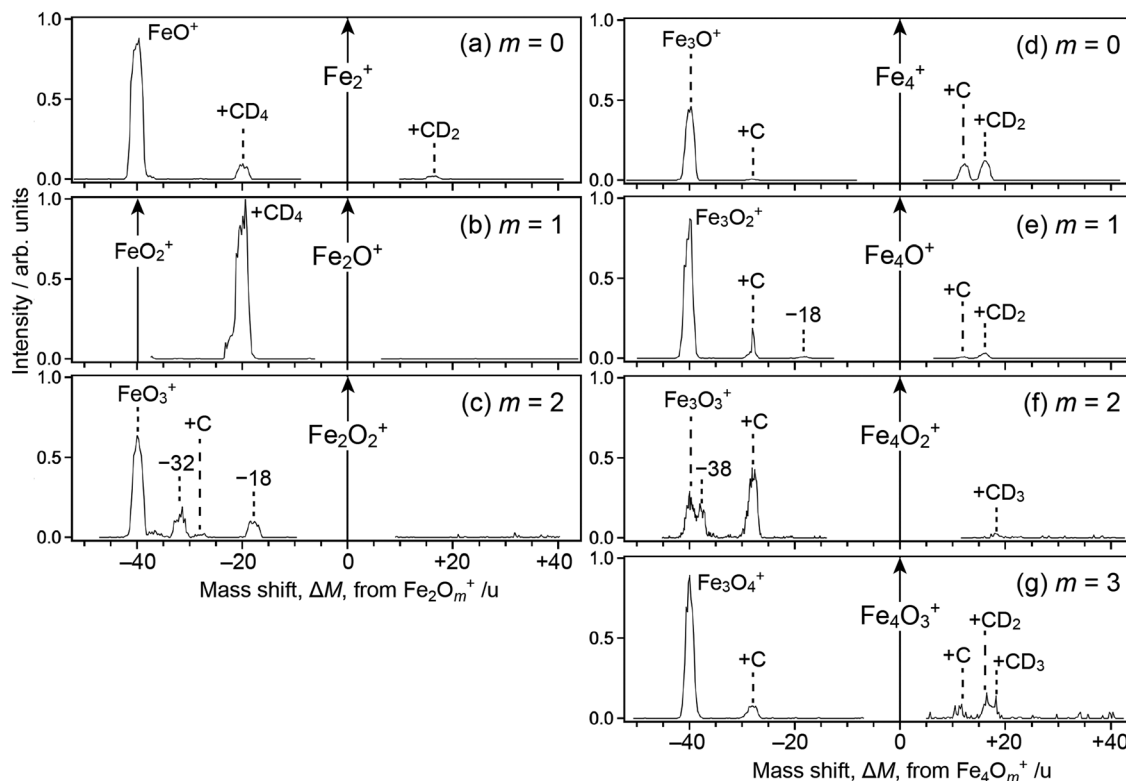
Fig. 2 Mass spectra of ions produced from the reaction of $Fe_nO_m^+$ and $Fe_{n-1}O_{m+1}Ar^+$ (n = 2 and 4) with CD_4. Reactant ions are (a)–(c) n = 2, m = 0–2; (d)–(g) n = 4, m = 0–3. The abscissa shows a mass shift, ΔM, from $Fe_nO_m^+$. Peaks are assigned to adducts to $Fe_nO_m^+$ in the $\Delta M \geq 0$ region, while adducts to $Fe_{n-1}O_{m+1}^+$ after desorption of Ar in the $\Delta M < 0$ region. Note that the following ions are excluded from recording due to saturation: Fe_2^+ in panel (a), Fe_2O^+ and FeO_2^+ in (b), $Fe_2O_2^+$ in (c), Fe_4^+ in (d), Fe_4O^+ in (e), $Fe_4O_2^+$ in (f), and $Fe_4O_3^+$ in (g). Several peaks marked by the value of ΔM are not simply assignable, originating probably from reactant ions containing more than two Ar atoms.

oxygen-poor clusters tend to exhibit higher reactivity. For example, the rate coefficients of O-free iron clusters, Fe_3^+ and Fe_4^+, are estimated to be 3×10^{-12} and 4×10^{-12} cm^3 s^{-1}, respectively. These values are consistent with the previous report;[78] note that the collision energies in the present experimental conditions for Fe_3^+ and Fe_4^+ are 1.0 and 0.8 eV in the center-of-mass frame, respectively. On the other hand, the present results estimate that the rate coefficients of monoxide clusters, Fe_3O^+ and Fe_4O^+, are 1×10^{-13} and 3×10^{-13} cm^3 s^{-1}, respectively; these values are an order of magnitude smaller than those of O-free iron clusters. The rate coefficients of $Fe_3O_2^+$, $Fe_3O_2^+$, $Fe_4O_2^+$ and $Fe_4O_3^+$, are even smaller by an order of magnitude than those of monoxide clusters. The extremely low reactivity of $Fe_2O_2^+$ is consistent with the previous report.[77] The rate coefficients obtained for CH_4 are shown in Fig. S2 of the ESI,† which are in the same order of magnitude as those for CD_4.

The rate coefficients of $Fe_nO_mAr^+$ obtained from the $\Delta M < 0$ region are shown in Fig. S3 of the ESI,† which were examined for CD_4; Fig. S3a and b (ESI†) show rate coefficients of dehydrogenation and those of CD_4 adsorption, respectively. The rate coefficients of CD_4 adsorption are about two orders of magnitude larger than those of the corresponding compositions shown in Fig. 3. This would be due to the effect of ligand exchange as discussed in Section 3.1. The rate coefficients of dehydrogenation are also higher than those of the

corresponding compositions. This result is also explainable by the effect of ligand exchange as discussed in the previous reaction study of $Rh_n^+Ar_m$ with CH_4.[80] The presence of Ar encourages CD_4 adsorption, causing dehydrogenation to proceed efficiently if the cluster–CD_4 complex retains a sufficient energy for methane activation.

3.3 Rapid methane loss in Mars' atmosphere

As described in Section 3.2, the rate coefficients of dehydrogenation by iron and iron-oxide clusters were obtained from the present reaction experiment. Here we consider the case that methane with an initial concentration of 2×10^9 cm^{-3} decreases by an order of magnitude in seven days ($\approx 6 \times 10^5$ s).[14] We also assume pseudo-first-order reaction kinetics by regarding the density of the iron-oxide clusters/particles as constant; we focus here on iron-oxide clusters because Mars' soil is rich in iron oxides. The pseudo-first-order rate equation, $-d[CH_4]/dt = kn[CH_4]$, is thus employed to estimate the number density n of the iron-oxide cluster from the rate coefficients k of methane dehydrogenation. Based on the value of $k = 1 \times 10^{-13}$ cm^3 s^{-1} obtained for Fe_3O^+ in the present study, we estimate that the presence of iron-oxide clusters/particles of 4×10^7 cm^{-3} ($\approx 10^{-7}$ Pa at -50 °C) would explain the mysterious loss of methane in Mars' atmosphere.

This journal is © the Owner Societies 2024

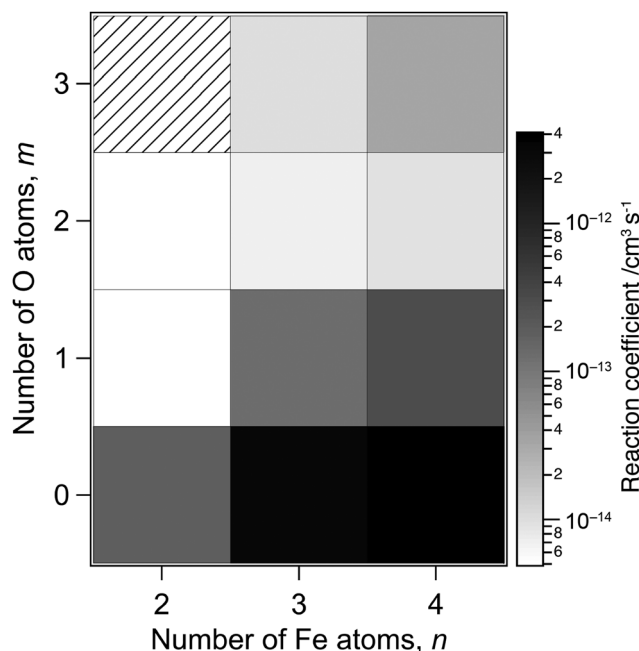*Phys. Chem. Chem. Phys.*, 2024, **26**, 14684–14690 | **14687**

Fig. 3 Rate coefficients of activation of CD$_4$ by Fe$_n$O$_m$$^+$ as a function of the numbers of iron, n, and oxygen atoms, m. White pixels at $(n,m) = (2,1)$ and $(2,2)$ indicate the compositions of the clusters, for which dehydrogenation of methane was not observed. The hatched pixel at $(n,m) = (2,3)$ represents an unexamined composition.

4 Conclusions

Gas-phase reaction experiments were performed on size-selected free iron and iron-oxide cluster cations, Fe$_n$O$_m$$^+$ (n = 2–4, $0 \leq m \leq n$), with methane. Dehydrogenation of methane was observed; larger and oxygen-poor clusters tend to exhibit higher reactivity. We also revealed that the presence of Ar as a weakly bound ligand promotes the adsorption and dehydrogenation of methane. Based on the rate coefficient of methane dehydrogenation determined in the present study, e.g., 1×10^{-13} cm^3 s^{-1} for Fe$_3$O$^+$, it is speculated that the presence of such iron-oxide clusters/particles in Mars' atmosphere at a density as low as 4×10^7 cm^{-3} ($\approx 10^{-7}$ Pa at -50 °C) is sufficient to explain the rapid loss of methane observed recently by the Curiosity rover. If ligand exchange with, for example, Ar were plausible, the required cluster/particle density could be even lower by about two orders of magnitude. The chemical process mediated by iron-oxide clusters/particles may play important roles in chemistry not only on Mars but also widely in space because most iron exists as compounds, typically iron oxides.[104]

Author contributions

M. A. contributed to conceptualization, investigation, formal analysis, writing – original draft, funding acquisition and project administration. S. K. contributed to investigation and formal analysis. Y. S. contributed to conceptualization and writing – review & editing. A. T. contributed to writing – review & editing and supervision.

Conflicts of interest

There are no conflicts to declare.

Acknowledgements

References

1 T. M. Steel and W. W. Duley, *Astrophys. J.*, 1987, **315**, 337–339.
2 R. van Boekel, M. Min, Ch Leinert, L. B. F. M. Waters, A. Richichi, O. Chesneau, C. Dominik, W. Jaffe, A. Dutrey, U. Graser, Th Henning, J. de Jong, R. Köhler, A. de Koter, B. Lopez, F. Malbet, S. Morel, F. Paresce, G. Perrin, Th Preibisch, F. Przygodda, M. Schöller and M. Wittkowski, *Nature*, 2004, **432**, 479–482.
3 J. A. Nuth III, N. M. Johnson and S. A. Manning, *Astrophys. J.*, 2008, **673**, L225–L228.
4 M. Arakawa, K. Kohara and A. Terasaki, *J. Phys. Chem. C*, 2015, **119**, 10981–10986.
5 M. Arakawa, K. Ando, S. Fujimoto, S. Mishra, G. Naresh Patwari and A. Terasaki, *Phys. Chem. Chem. Phys.*, 2018, **20**, 13974–13982.
6 M. Arakawa, M. Horioka, K. Minamikawa, T. Kawano and A. Terasak, *J. Phys. Chem. C*, 2020, **124**, 26881–26888.
7 S. M. Lang and T. M. Bernhardt, *Phys. Chem. Chem. Phys.*, 2012, **14**, 9255–9269.
8 A. C. Reber, S. Paranthaman, P. A. Clayborne, S. N. Khanna and A. W. Castleman, Jr., *ACS Nano*, 2008, **2**, 1729–1737.
9 J. M. Guiu, B.-A. Ghejan, T. M. Bernhardt, J. M. Bakker, S. M. Lang and S. T. Bromley, *ACS Earth Space Chem.*, 2022, **6**, 2465–2470.
10 T. Studemund, K. Pollow, M. Förstel and O. Dopfer, *Phys. Chem. Chem. Phys.*, 2023, **25**, 17609–17618.
11 M. Arakawa, R. Yamane and A. Terasaki, *J. Phys. Chem. A*, 2016, **120**, 139–144.
12 M. Arakawa, T. Omoda and A. Terasaki, *J. Phys. Chem. C*, 2017, **121**, 10790–10795.
13 M. Arakawa, D. Okada, S. Kono and A. Terasaki, *J. Phys. Chem. A*, 2020, **124**, 9751–9756.
14 C. R. Webster, P. R. Mahaffy, S. K. Atreya, J. E. Moores, G. J. Flesch, C. Malespin, C. P. McKay, G. Martinez, G. L. Smith and J. Martin-Torres, *Science*, 2018, **360**, 1093–1096.
15 Y. Luo, M. Mischna, J. Lin, B. Fasoli, X. Cai and Y. Yung, *Earth Space Sci.*, 2021, **8**(11), e2021EA001915.

14688 | *Phys. Chem. Chem. Phys.*, 2024, **26**, 14684–14690

This journal is © the Owner Societies 2024

16 A. A. Pavlov, J. Johnson, R. Garcia-Sanchez, A. Siguelnitzky, C. Johnson, J. Davis, S. Guzewich and P. Misra, *J. Geophys. Res. Planets*, 2024, **129**, e2023JE007841.

17 P. L. Whelley and R. Greeley, *J. Geophys. Res.*, 2008, **213**, E07002.

18 C. Ganino, G. Libourel, A. M. Nakamura, S. Jacomet, O. Tottereau and P. Michel, *Meteorit. Planet. Sci.*, 2018, **53**(11), 2306–2326.

19 A. C. Rosenzweig, P. Nordlund, P. M. Takahara, C. A. Frederick and S. J. Lippard, *Nature*, 1993, **366**, 537–543.

20 A. C. Rosenzweig, P. Nordlund, P. M. Takahara, C. A. Frederick and S. J. Lippard, *Chem. Biol.*, 1995, **2**, 409–418.

21 M. Merkx, D. A. Kopp, M. H. Sazinsky, J. L. Blazyk, J. Müller and S. J. Lippard, *Angew. Chem. Int. Ed.*, 2001, **40**, 2782–2807.

22 L. Shu, J. C. Nesheim, K. Kauffmann, E. Münck, J. D. Lipscomb and L. Que Jr., *Science*, 1997, **275**, 515–518.

23 B. J. Brazeau, R. N. Austin, C. Tarr, J. T. Groves and J. D. Lipscomb, *J. Am. Chem. Soc.*, 2001, **123**, 11831–11837.

24 K. Yoshizawa, *Acc. Chem. Res.*, 2006, **39**, 375–382.

25 K. Yoshizawa and R. Hoffmann, *Inorg. Chem.*, 1996, **25**, 2409–2410.

26 K. Yoshizawa, T. Ohta, T. Yamabe and R. Hoffmann, *J. Am. Chem. Soc.*, 1997, **26**, 12311–12321.

27 K. Yoshizawa, T. Ohta, Y. Shiota and T. Yamabe, *Chem. Lett.*, 1997, 1213–1214.

28 P. E. M. Siegbahn and R. H. Crabtree, *J. Am. Chem. Soc.*, 1997, **119**, 3103–3113.

29 P. E. M. Siegbahn, *J. Biol. Inorg. Chem.*, 2001, **6**, 27–45.

30 K. Yoshizawa, T. Ohta and T. Yamabe, *Bull. Chem. Soc. Jpn.*, 1998, **119**, 1899–1909.

31 H. Basch, K. Mogi, D. G. Musaev and K. Morokuma, *J. Am. Chem. Soc.*, 1999, **121**, 7249–7256.

32 B. D. Dunietz, M. D. Beachy, Y. Cao, D. A. Whittington and S. J. Lippard, *J. Am. Chem. Soc.*, 2000, **122**, 2828–2839.

33 K. Yoshizawa and T. Yumura, *Chem. – Eur. J.*, 2003, **9**, 2347–2358.

34 S.-P. Huang, Y. Shiota and K. Yoshizawa, *Dalton Trans.*, 2013, **42**, 1011–1023.

35 K. Yoshizawa, *Bull. Chem. Soc. Jpn.*, 2013, **86**, 1083–1116.

36 M. Barona, C. A. Gaggioli, L. Gagliardi and R. Q. Snurr, *J. Phys. Chem. A*, 2020, **124**, 1580–1592.

37 D. Schröder and H. Schwarz, *Angew. Chem., Int. Ed. Engl.*, 1990, **29**, 1433–1434.

38 D. Schröder, A. Fiedler, J. Hrušák and H. Schwarz, *J. Am. Chem. Soc.*, 1992, **114**, 1215–1222.

39 D. Schröder and H. Schwarz, *Angew. Chem., Int. Ed. Engl.*, 1995, **34**, 1973–1995.

40 D. Schröder, H. Schwarz, D. E. Clemmer, Y. Chen, P. B. Armentrout, V. I. Baranov and D. K. Böhme, *Int. J. Mass Spectrom. Ion Processes*, 1997, **161**, 175–191.

41 D. Schröder and H. Schwarz, *Proc. Natl. Acad. Sci. U. S. A.*, 2008, **105**, 18114–18119.

42 K. Yoshizawa, Y. Shiota and T. Yamabe, *Chem.–Eur. J.*, 1997, **3**, 1160–1169.

43 K. Yoshizawa, Y. Shiota and T. Yamabe, *J. Am. Chem. Soc.*, 1998, **120**, 564–572.

44 G. Altinay, M. Citir and R. B. Metz, *J. Phys. Chem. A*, 2010, **114**, 5104–5112.

45 K. Yoshizawa, Y. Shiota and T. Yamabe, *Organometallics*, 1998, **17**, 2825–2831.

46 K. Yoshizawa, Y. Shiota and T. Yamabe, *J. Chem. Phys.*, 1999, **111**, 538–545.

47 Y. Shiota and K. Yoshizawa, *J. Am. Chem. Soc.*, 2000, **122**, 12317–12326.

48 K. Yoshizawa, Y. Shiota, Y. Kagawa and T. Yamabe, *J. Phys. Chem. A*, 2000, **104**, 2552–2561.

49 Y. Shiota and K. Yoshizawa, *J. Chem. Phys.*, 2003, **118**, 5872–5879.

50 Y. Wang, X. Sun, J. Zhang and Jilai Li, *J. Phys. Chem. A*, 2017, **121**, 3501–3514.

51 T. Zubatiuk, G. Hill, D. Leszczynska, M. Fan, A. H. Rony and J. Leszczynski, *Chem. Phys. Lett.*, 2018, **706**, 708–714.

52 Q. Sun, Z. Li, A. Du, J. Chen, Z. Zhu and S. C. Smith, *Fuel*, 2012, **96**, 291–297.

53 S. Chiodo, I. Rivalta, M. del Carmen Michelini, N. Russo, E. Sicilia and J. M. Ugalde, *J. Phys. Chem. A*, 2006, **110**, 12501–12511.

54 Q. Sun, Z. Li, M. Wang, A. Du and S. C. Smith, *Chem. Phys. Lett.*, 2012, **550**, 41–46.

55 A. Fiedler, J. Hrušák, W. Koc and H. Schwarz, *Chem. Phys. Lett.*, 1993, **211**, 242–248.

56 A. Fiedler, D. Schröder, S. Shaik and H. Schwarz, *J. Am. Chem. Soc.*, 1994, **116**, 10734–10741.

57 Z. Cao, M. Duran and M. Solà, *Chem. Phys. Lett.*, 1997, **274**, 411–421.

58 A. T. García-Sosa and M. Castro, *Int. J. Quantum Chem.*, 2000, **80**, 307–319.

59 G. L. Gutsev, S. N. Khanna, B. K. Rao and P. Jena, *J. Phys. Chem. A*, 1999, **103**, 5812–5822.

60 H. Shiroishi, T. Oda, I. Hamada and N. Fujima, *Polyhedron*, 2005, **24**, 2472–2476.

61 N. M. Reilly, J. U. Reveles, G. E. Johnson, S. N. Khanna and A. W. Castleman, Jr., *J. Phys. Chem. A*, 2007, **111**, 4158–4166.

62 H. Shiroishi, T. Oda, I. Hamada and N. Fujima, *Eur. Phys. J. D*, 2003, **24**, 85–88.

63 N. O. Jones, B. V. Reddy, F. Rasouli and S. N. Khanna, *Phys. Rev. B: Condens. Matter Mater. Phys.*, 2005, **72**, 165411.

64 G. L. Gutsev, K. G. Belay, L. G. Gutsev and B. R. Ramachandra, *Comput. Mater. Sci.*, 2017, **137**, 134–143.

65 S. Yin, W. Xue, X.-L. Ding, W.-G. Wang, S.-G. He and M.-F. Ge, *Int. J. Mass Spectrom.*, 2009, **281**, 72–78.

66 X.-L. Ding, W. Xue, Y.-P. Ma, Z.-C. Wang and S.-G. He, *J. Phys. Chem.*, 2009, **130**, 014303.

67 A. Erlebach, C. Hühn, R. Jana and M. Sierka, *Phys. Chem. Chem. Phys.*, 2014, **16**, 26421–26426.

68 R. Mejia-Olvera, J. U. Reveles, S. M. Pacheco-Ortín and J. Santoyo-Salazar, *Chem. Phys. Lett.*, 2018, **706**, 494–500.

69 R. Logemann, G. A. de Wijs, M. I. Katsnelson and A. Kirilyuk, *Phys. Rev. B: Condens. Matter Mater. Phys.*, 2015, **92**, 144427.

This journal is © the Owner Societies 2024

Phys. Chem. Chem. Phys., 2024, **26**, 14684–14690 | **14689**

70 S. López, A. H. Romero, J. Mejía-López, J. Mazo-Zuluaga and J. Restrepo, *Phys. Rev. B: Condens. Matter Mater. Phys.*, 2009, **80**, 085107.

71 Q. Wang, Q. Sun, M. Sakurai, J. Z. Yu, B. L. Gu, K. Sumiyama and Y. Kawazoe, *Phys. Rev. B: Condens. Matter Mater. Phys.*, 1999, **59**, 12672–12677.

72 Q. Sun, Q. Wang, K. Parlinski, J. Z. Yu, Y. Hashi, X. G. Gong and Y. Kawazoe, *Phys. Rev. B: Condens. Matter Mater. Phys.*, 2000, **61**, 5781–5785.

73 K. Palotás, A. N. Andriotis and A. Lappas, *Phys. Rev. B: Condens. Matter Mater. Phys.*, 2010, **81**, 075403.

74 K. Ohshimo, T. Komukai, R. Moriyama and F. Misaizu, *J. Phys. Chem. A*, 2014, **118**, 3899–3905.

75 K. S. Molek, C. Anfuso-Cleary and M. A. Duncan, *J. Phys. Chem. A*, 2008, **112**, 9238–9247.

76 M. Li, S.-R. Liu and P. B. Armentrout, *J. Phys. Chem.*, 2009, **131**, 144310.

77 P. Jackson, J. N. Harvey, D. Schröder and H. Schwarz, *Int. J. Mass Spectrom.*, 2001, **204**, 223–245.

78 R. Liyanage, X.-G. Zhang and P. B. Armentrout, *J. Chem. Phys.*, 2001, **115**, 9747–9763.

79 F. Liu, X.-G. Zhang, R. Liyanage and P. B. Armentrout, *J. Chem. Phys.*, 2004, **121**, 10976–10990.

80 G. Albert, C. Berg, M. Beyer, U. Achatz, S. Joos, G. Niedner-Schatteburg and V. E. Bondybey, *Chem. Phys. Lett.*, 1997, **268**, 235–241.

81 S. M. Lang and T. M. Bernhardt, *Faraday Disc.*, 2011, **152**, 337–351.

82 S. M. Lang, A. Frank and T. M. Bernhardt, *Catal. Sci. Technol.*, 2013, **3**, 2926–2933.

83 S. M. Lang, A. Frank and T. M. Bernhardt, *J. Phys. Chem. C*, 2013, **117**, 9791–9800.

84 J. F. Eckhard, T. Masubuchi, M. Tschurl, R. N. Barnett, U. Landman and U. Heiz, *J. Phys. Chem. A*, 2021, **125**, 5289–5302.

85 S. M. Lang, T. M. Bernhardt, R. N. Barnett and U. Landman, *Angew. Chem., Int. Ed.*, 2010, **49**, 980–983.

86 S. M. Lang, T. M. Bernhardt, R. N. Barnett and U. Landman, *J. Phys. Chem. C*, 2011, **115**, 6788–6795.

87 H.-F. Li, Z.-Y. Li, Q.-Y. Liu, X.-N. Li, Y.-X. Zhao and S.-G. He, *J. Phys. Chem. Lett.*, 2015, **6**, 2287–2291.

88 S. Hirabayashi and M. Ichihashi, *J. Phys. Chem. A*, 2020, **124**, 5274–5279.

89 Z.-C. Wang, T. Weiske, R. Kretschmer, M. Schlangen, M. Kaupp and H. Schwarz, *J. Am. Chem. Soc.*, 2011, **133**, 16930–16937.

90 C.-M. Sun, G.-P. Wei, Y. Yang and Y.-X. Zhao, *J. Phys. Chem. A*, 2024, **128**, 1218–1225.

91 M. Citir, G. Altinay, G. Austein-Miller and R. B. Metz, *J. Chem. Phys. A*, 2010, **114**, 11322–11329.

92 M. A. Ashraf, Ch. W. Copeland, A. Kocak, A. R. McEnroe and R. B. Metz, *Phys. Chem. Chem. Phys.*, 2015, **17**, 25700–25704.

93 C. W. Copeland, M. A. Ashraf, E. M. Boyle and R. B. Metz, *J. Phys. Chem. A*, 2017, **121**, 2132–2137.

94 O. V. Lushchikova, S. Reijmer, P. B. Armentrout and J. M. Bakker, *J. Am. Soc. Mass Spectrom.*, 2022, **33**, 1393–1400.

95 J. Lengyel, N. Levin, F. J. Wensink, O. V. Lushchikova, R. N. Barnett, U. Landman, U. Heiz, J. M. Bakker and M. Tschurl, *Angew. Chem., Int. Ed.*, 2020, **59**, 23631–23635.

96 D. J. Harding, C. Kerpal, G. Meijer and A. Fielicke, *Angew. Chem., Int. Ed.*, 2012, **51**, 817–819.

97 S. M. Lang, T. M. Bernhardt, V. Chernyy, J. M. Bakker, R. N. Barnett and U. Landman, *Angew. Chem., Int. Ed.*, 2017, **56**, 13406–13410.

98 A. Terasaki, T. Majima and T. Kondow, *J. Chem. Phys.*, 2007, **127**, 231101.

99 M. Arakawa, K. Kohara, T. Ito and A. Terasaki, *Eur. Phys. J. D*, 2013, **67**, 80.

100 H. Haberland, M. Karrais, M. Mall and Y. Thurner, *J. Vac. Sci. Technol., A*, 1992, **10**, 3266.

101 T. Ito, K. Egashira, K. Tsukiyama and A. Terasaki, *Chem. Phys. Lett.*, 2012, **538**, 19–23.

102 J. B. Griffin and P. B. Armentrout, *J. Chem. Phys.*, 1998, **108**, 8062–8074.

103 G. Gioumousis and D. P. Stevenson, *J. Chem. Phys.*, 1958, **29**, 294–299.

104 Y. Kimura, K. K. Tanaka, T. Nozawa, S. Takeuchi and Y. Inatomi, *Sci. Adv.*, 2017, **3**, e1601992.

14690 | *Phys. Chem. Chem. Phys.*, 2024, **26**, 14684–14690

This journal is © the Owner Societies 2024